Supplementary Material

Analysis

Quasi-linkage equilibrium analyses were also performed relaxing the assumption that ψ_H and ψ_P were near one. The main difference is that the departure from Hardy-Weinberg at the A locus (denoted $F_{A,H}$ in hosts and $F_{A,P}$ in parasites) then becomes substantial (see table S1 for the full expressions for $F_{A,H}$ and $F_{A,P}$). Full expressions for $\bar{w}_{\text{diff}}$ are given in table S2. Because $F_{A,H}$ and $F_{A,P}$ are still on the same order as the strength of selection, however, these terms again drop out when we assume selection is weak and focus on the leading order terms.

Simulations

We summarize here a number of extensions to our model that were examined using simulations. Simulations matched our analytical predictions when mutation rates were high and cycles were small in every case, except when we considered more alleles at the interaction locus (discussed below). Where discrepancies were observed, they could be explained by accounting for the allele frequency dynamics (i.e., calculating δ_H and δ_P in every generation and using these in table 3). Also note that in each case, any shifts that did occur did not affect our main conclusions that parasitism is more likely to evolve under MAM than IMAM (but see results with three alleles) and that haploid parasites are more likely to evolve higher parasitism levels than diploids.

- Figure S1: simulations of MAM/IMAM comparing low and high mutation rates ($\mu = 10^{-1}$ versus $\mu = 10^{-5}$).
- Figure S2: same as figure S1, except with selection in hosts reduced ($\alpha_H = 0.01$).
- Figure S3: same as figure S1, except with stronger selection in hosts ($\alpha_H = 0.5$) and in parasites ($0 < \alpha_P < 1$).

- Figure S4: same as figure S1, except with population sizes of 10^3 in both species.
- Figure S5: same as figure S1, except with some hosts reproducing asexually ($\psi_H = 0.2$). Mutations were introduced at the same rate during sexual and asexual reproduction.
- Figure S6: same as figure S1, except with different generation times in hosts and parasites. Only 20% of hosts reproduced at each time step, and thus had, on average, a generation time five times that of parasites. Mutations were introduced only during reproduction, so that hosts had 20% the rate of mutations per unit times as parasites.
- Figure S7: same as figure S1, except with three alleles at the A-locus in each species. See below for a more detailed description of this case.
- Figure S8: evolutionary convergent level of parasitism in the GFG with conditional costs to virulence.
- Figure S9: evolutionary convergent level of parasitism in the GFG with unconditional costs to virulence.
- Figure S10: same as figure S9, except with population sizes of 10^3 in both species.

Three alleles at the interaction locus

Qualitative shifts occurred in all cases when there were three alleles at the A-locus. These shifts could be described analytically by developing the model explicitly for multiple alleles. With MAM, the region where parasitism evolved shrunk with more alleles, whereas with IMAM it grew (figure S7). This is because with MAM the heterozygous parasites can infect a lower proportion of the genotypes when there are more alleles present, whereas the opposite is true in the IMAM. For example, with three or more alleles, a host

homozygous for an allele not present in a heterozygous parasite cannot be invaded by that parasite in the matching-alleles model, whereas when there are only two alleles a heterozygous parasite can invade all possible host genotypes. In the inverse-matching-alleles model the opposite is true, with new host genotypes providing additional targets for heterozygous parasites (in the case of two alleles, heterozygous parasites cannot invade any host genotypes, but with three they can invade hosts homozygous for the allele that the parasite does not carry). Large cycles had the same effect with three alleles as they did with two, reducing and enlarging the same regions (figure S7).

Model	Host ploidy	Parasite ploidy	$\bar{w}_{\text{diff}}$
MAM/IMAM	1	2	$F_{A,P} = (1/4 - \delta_P^2)^2 f_{mm}(\alpha_P + \beta_P)(1 - \psi_P)/\psi_P$
	2	1	$F_{A,H} = (1/4 - \delta_H^2)^2 f_m \alpha_H (1 - \psi_H)/\psi_H$
	2	2	$F_{A,H} = (1/4 - \delta_H^2)^2 (3/4 - \delta_P^2) 2 f_{mm} \alpha_H (1 - \psi_H)/\psi_H$,
			$F_{A,P} = (1/4 - \delta_P^2)^2 (1/4 + \delta_H^2 + F_{A,H}) 2 f_{mm}(\alpha_P + \beta_P)(1 - \psi_P)/\psi_P$
GFG	1	2	$F_{A,P} = (1/4 - \delta_P^2)^2 (c_{P,u} + f_{mm} c_{P,c} - f_{mm}(\alpha_P + \beta_P)(1/2 + \delta_H))(1 - \psi_P)/\psi_P$
	2	1	$F_{A,H} = (1/4 - \delta_H^2)^2 (c_H - f_m \alpha_H (1/2 - \delta_P))(1 - \psi_H)/\psi_H$
	2	2	$F_{A,H} = (1/4 - \delta_H^2)^2 (c_H - f_{mm} \alpha_H (1/2 - \delta_P)^2)(1 - \psi_H)/\psi_H$,
			$F_{A,P} = (1/4 - \delta_P^2)^2 (c_{P,u} + f_{mm} c_{P,c} + f_{mm}(\alpha_P + \beta_P)(\delta_H^2 - \delta_H - 3/4))(1 - \psi_P)/\psi_P$

Table S1: Equations for $F_{A,H}$ and $F_{A,P}$ when ψ_H and ψ_P are not assumed to be near 1.

Model	Host ploidy	Parasite ploidy	$\bar{w}_{\text{diff}}$
MAM	1	1	$(\alpha_P - \beta_P)/2 + (\alpha_P + \beta_P)(2\delta_H\delta_P)$
	1	2	$(\alpha_P - 3\beta_P)/4 + (\alpha_P + \beta_P)(2\delta_H\delta_P + \delta_P^2 + F_{A,P})$
	2	1	$(3\alpha_P - \beta_P)/4 + (\alpha_P + \beta_P)(2\delta_H\delta_P - \delta_H^2 - F_{A,H})$
	2	2	$(5\alpha_P - 3\beta_P)/8 + (\alpha_P + \beta_P)[4\delta_H\delta_P(1 + \delta_H\delta_P) - 3\delta_H^2 + \delta_P^2 +$ $(1 + 4\delta_H^2)F_{A,P} - (3 - 4\delta_P^2)F_{A,H} + 4F_{A,P}F_{A,H}]/2$
IMAM	1	1	$(\alpha_P - \beta_P)/2 - (\alpha_P + \beta_P)(2\delta_H\delta_P)$
	1	2	$(\alpha_P - 3\beta_P)/4 - (\alpha_P + \beta_P)(2\delta_H\delta_P - \delta_P^2 - F_{A,P})$
	2	1	$(\alpha_P - 3\beta_P)/4 - (\alpha_P + \beta_P)(2\delta_H\delta_P - \delta_H^2 - F_{A,H})$
	2	2	$(\alpha_P - 7\beta_P)/8 - (\alpha_P + \beta_P)[4\delta_H\delta_P(1 - \delta_H\delta_P) - \delta_H^2 - \delta_P^2 -$ $(1 + 4\delta_H^2)F_{A,P} - (1 + 4\delta_P^2)F_{A,H} - 4F_{A,H}F_{A,P}/]2$
GFG	1	1	$(3\alpha_P - \beta_P)/4 + (\alpha_P + \beta_P)(\delta_P - \delta_H(1 - 2\delta_P))/2 - c_{P,c}(1 + 2\delta_P)$
	1	2	$(7\alpha_P - \beta_P)/8 + (\alpha_P + \beta_P)(2(1 + 2\delta_H)(1 - \delta_P)\delta_P - \delta_H - 2(2\delta_H + 1)F_{A,P})/4 -$ $c_{P,c}(3/4 + (1 - \delta_P)\delta_P - F_{A,P})$
	2	1	$(5\alpha_P - 3\beta_P)/8 + (\alpha_P + \beta_P)(3\delta_P + 2(1 - 2\delta_P)(\delta_H^2 - \delta_H + F_{A,H}))/4 - c_{P,c}(1 + 2\delta_P)$
	2	2	$(13\alpha_P - 3\beta_P)/16 + (\alpha_P + \beta_P)[\delta_H^2(1 - 2\delta_P)^2 - \delta_H(1 - 2\delta_P)^2 - 3(\delta_P - 1)\delta_P +$ $(1 - 2\delta_P)^2F_{A,H} + (4\delta_H^2 - 4\delta_H - 3)F_{A,P} + 4F_{A,H}F_{A,P}]/4 -$ $c_{P,c}(3/4 + (1 - \delta_P)\delta_P + F_{A,P})$

Table S2: Full equations for $\bar{w}_{\text{diff}} = \bar{w}_M - \bar{w}_m$, without assuming high levels of sexual reproduction in either species (e.g., without assuming ψ_H and ψ_P are on the order of $1 - \epsilon$).

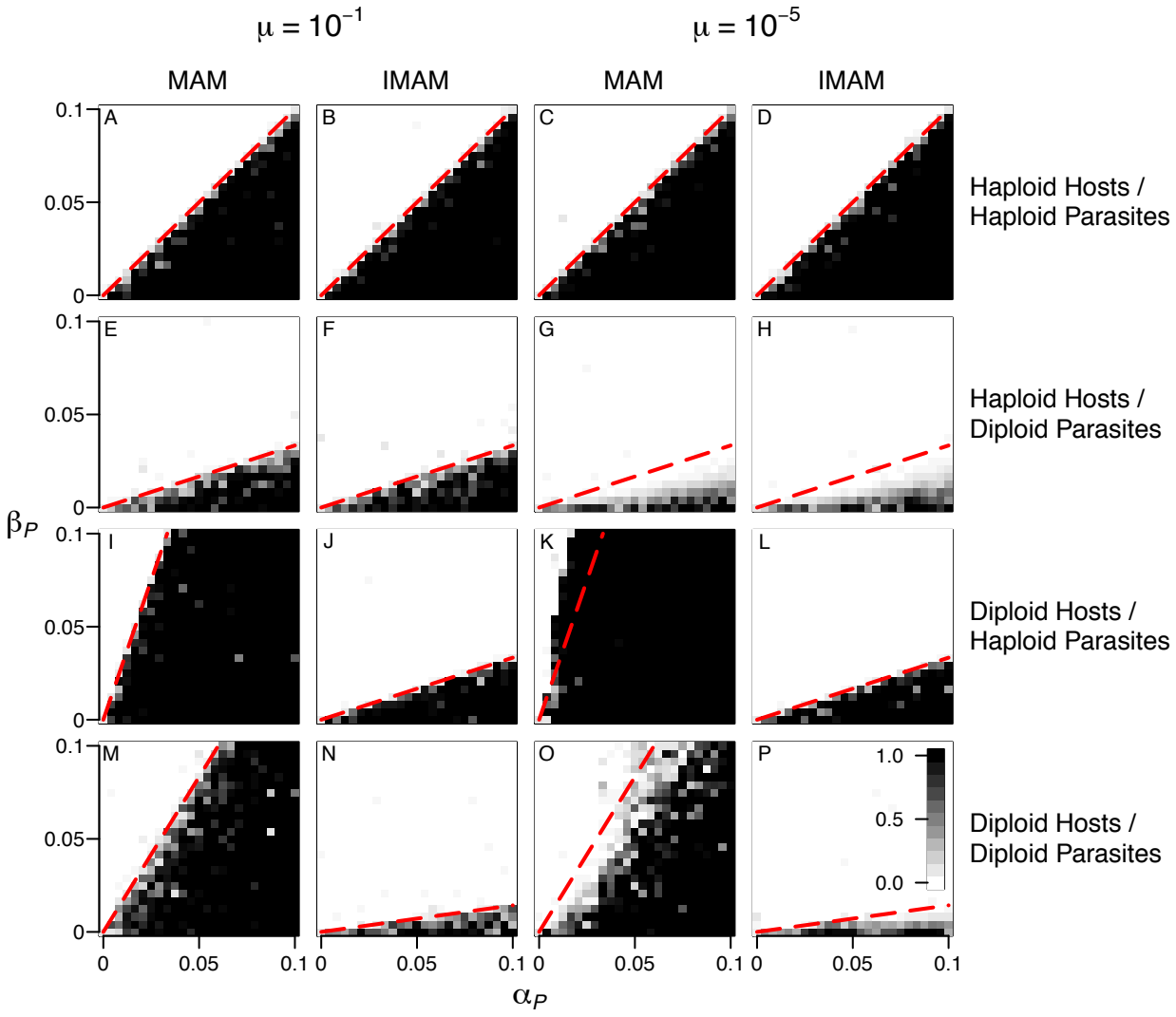

Figure S1: Evolutionary convergent level of parasitism (f) in MAM and IMAM. Right two columns are identical to figure 4. Left two columns report simulations with $\mu = 10^{-1}$ for comparison. Dashed red lines denote the analytical invasion condition assuming small cycles (table 4). Cells are shaded based on the mean level of parasitism present in the population after 10^6 generations of evolution in a single simulation (darker = higher, see grayscale in panel P). Parameters were $\alpha_H = 0.05, \psi_H = \psi_P = 1, r = 0.5$ and population sizes of 10^6 in both species.

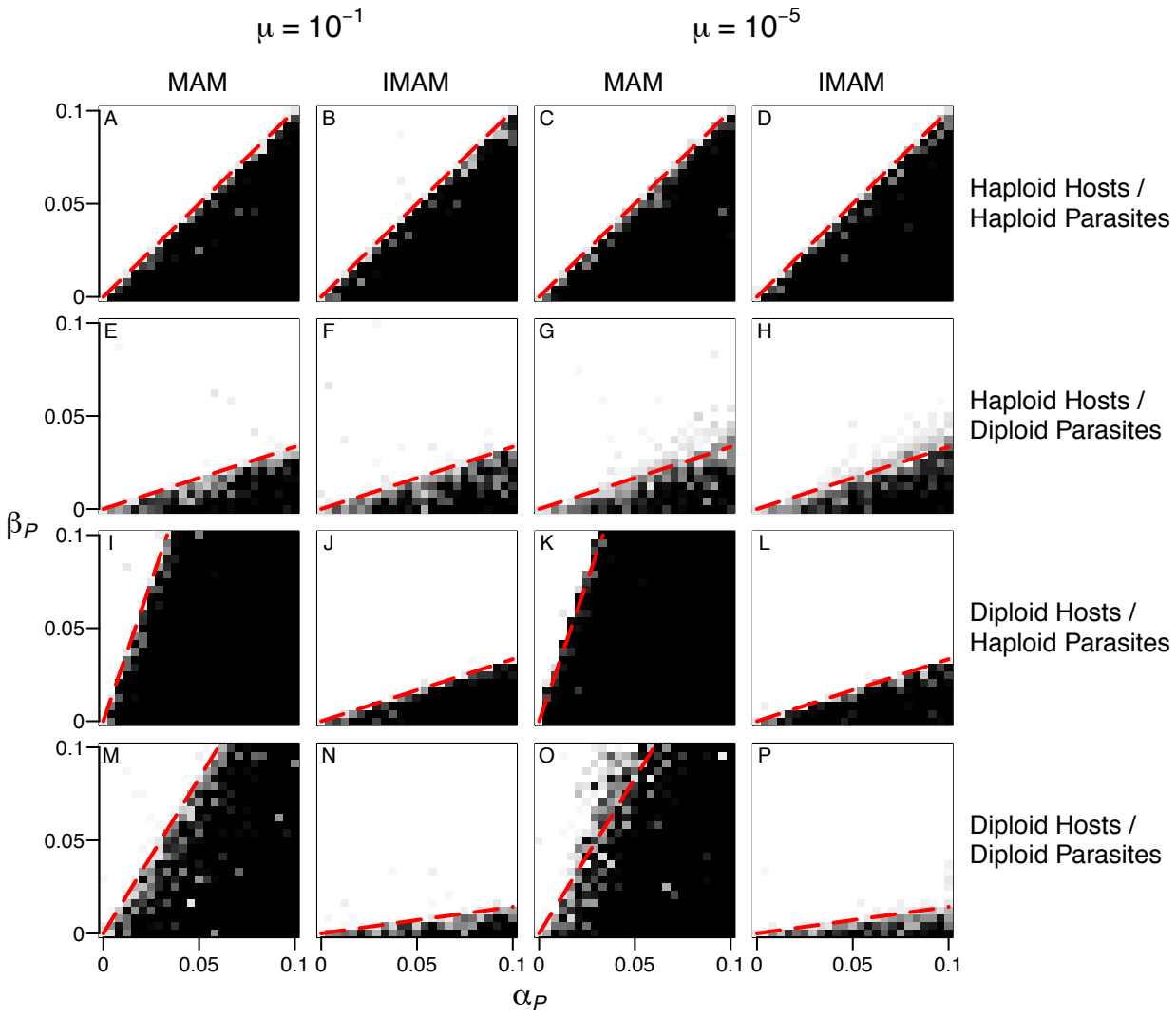

Figure S2: Same as figure S1, except with $\alpha_H = 0.01$.

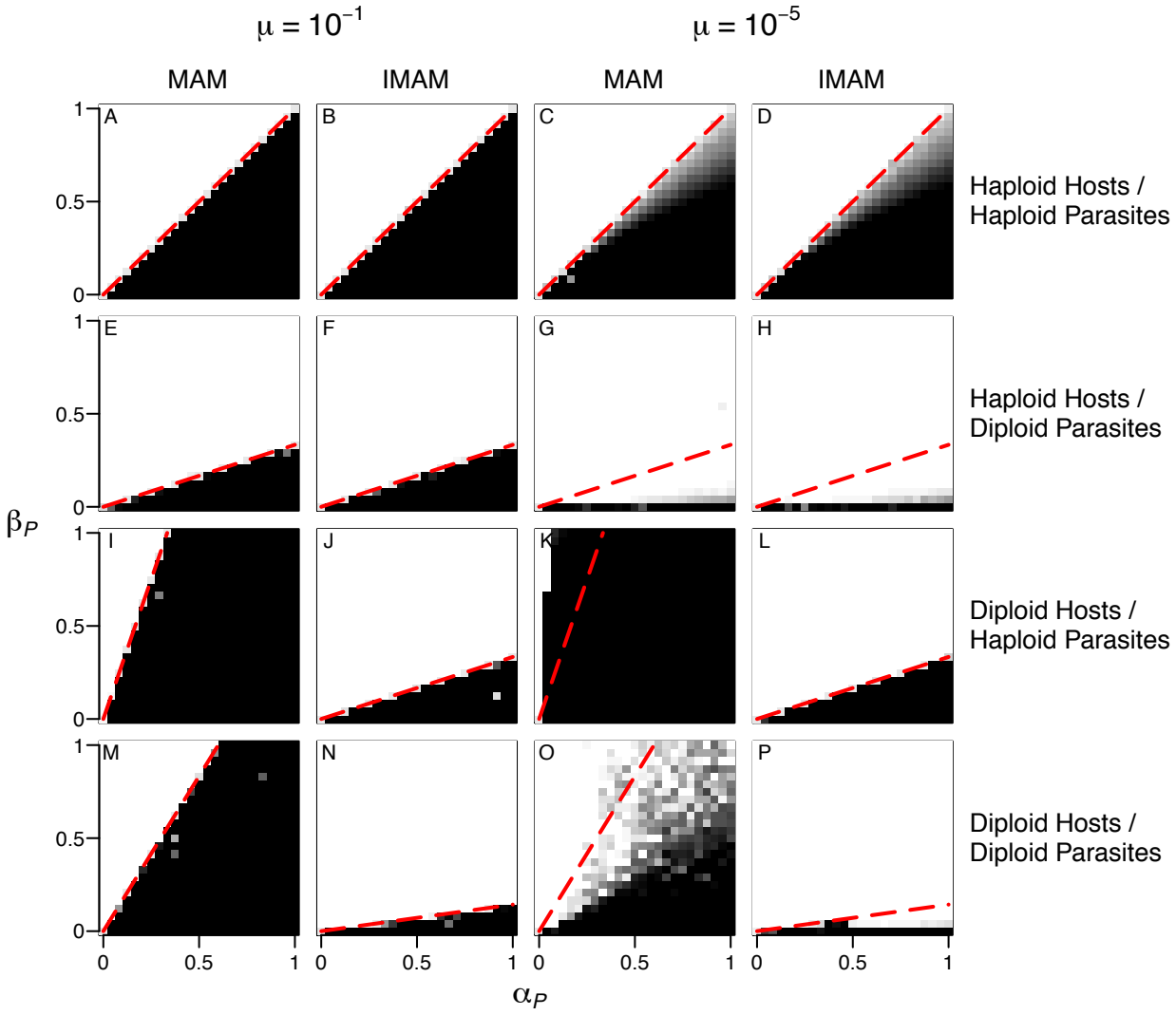

Figure S3: Same as figure S1, except with stronger selection in hosts ($\alpha_H = 0.5$) and in parasites (note change in axes ranges).

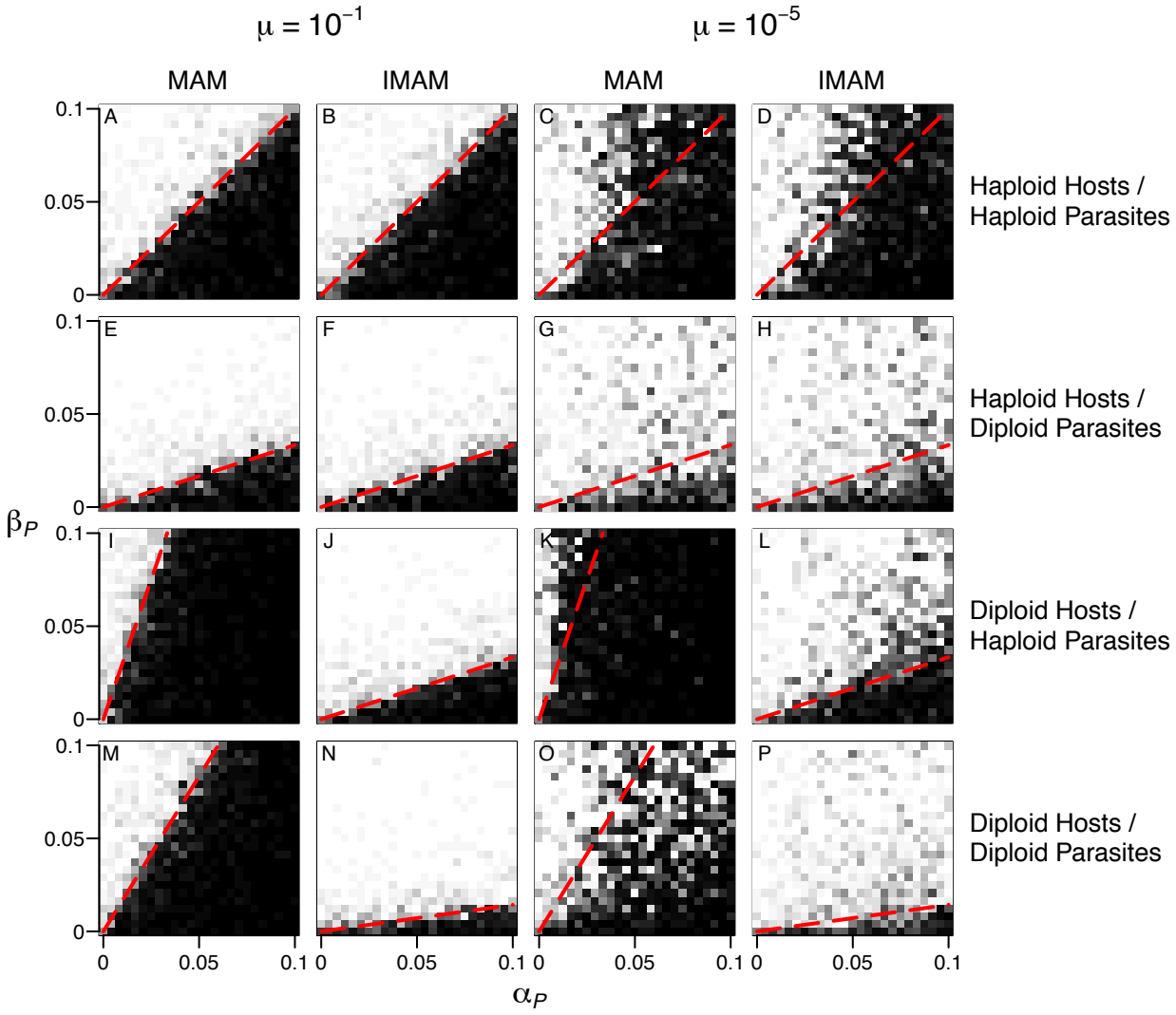

Figure S4: Same as figure S1, except with population sizes of 10^3 in both species.

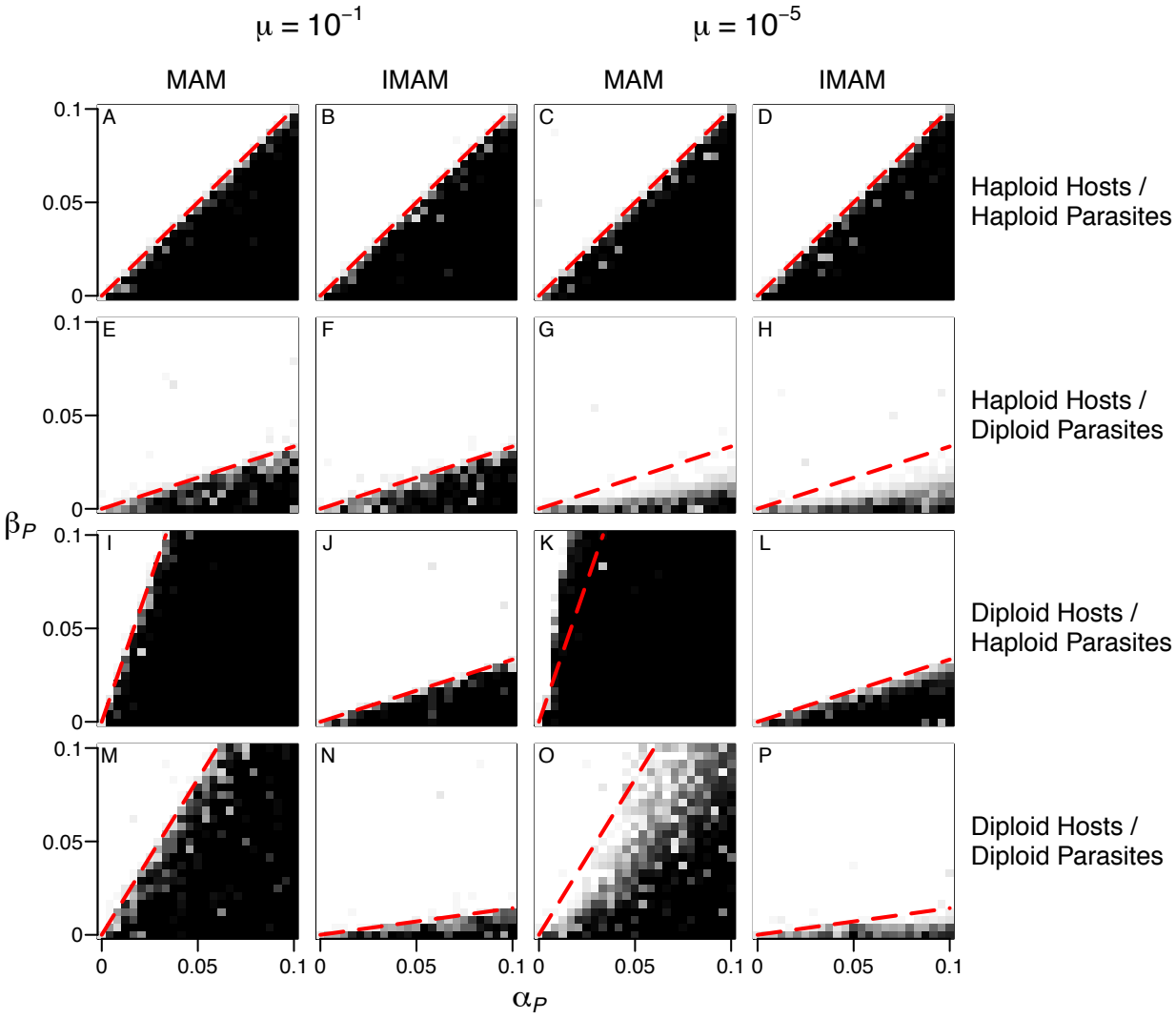

Figure S5: Same as figure S1, except with some hosts reproducing asexually ($\psi_H = 0.2$). Mutations were introduced at the same rate during sexual and asexual reproduction.

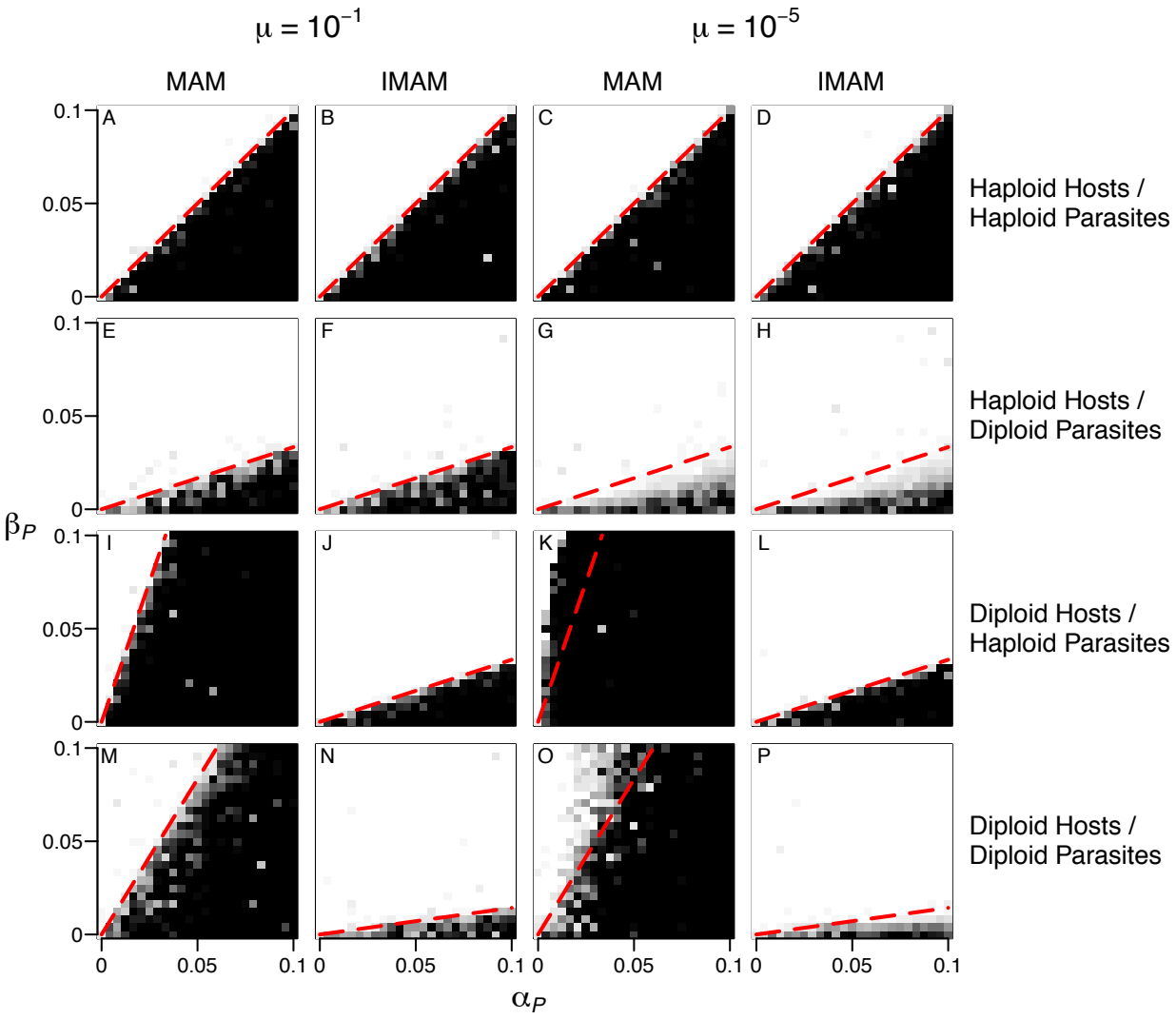

Figure S6: Same as figure S1, except with different generation times in hosts and parasites. Only 20% of hosts reproduced at each time step, and thus had, on average, a generation time five times that of parasites. Mutations were introduced only during reproduction, so that hosts had 20% the rate of mutations per unit times as parasites.

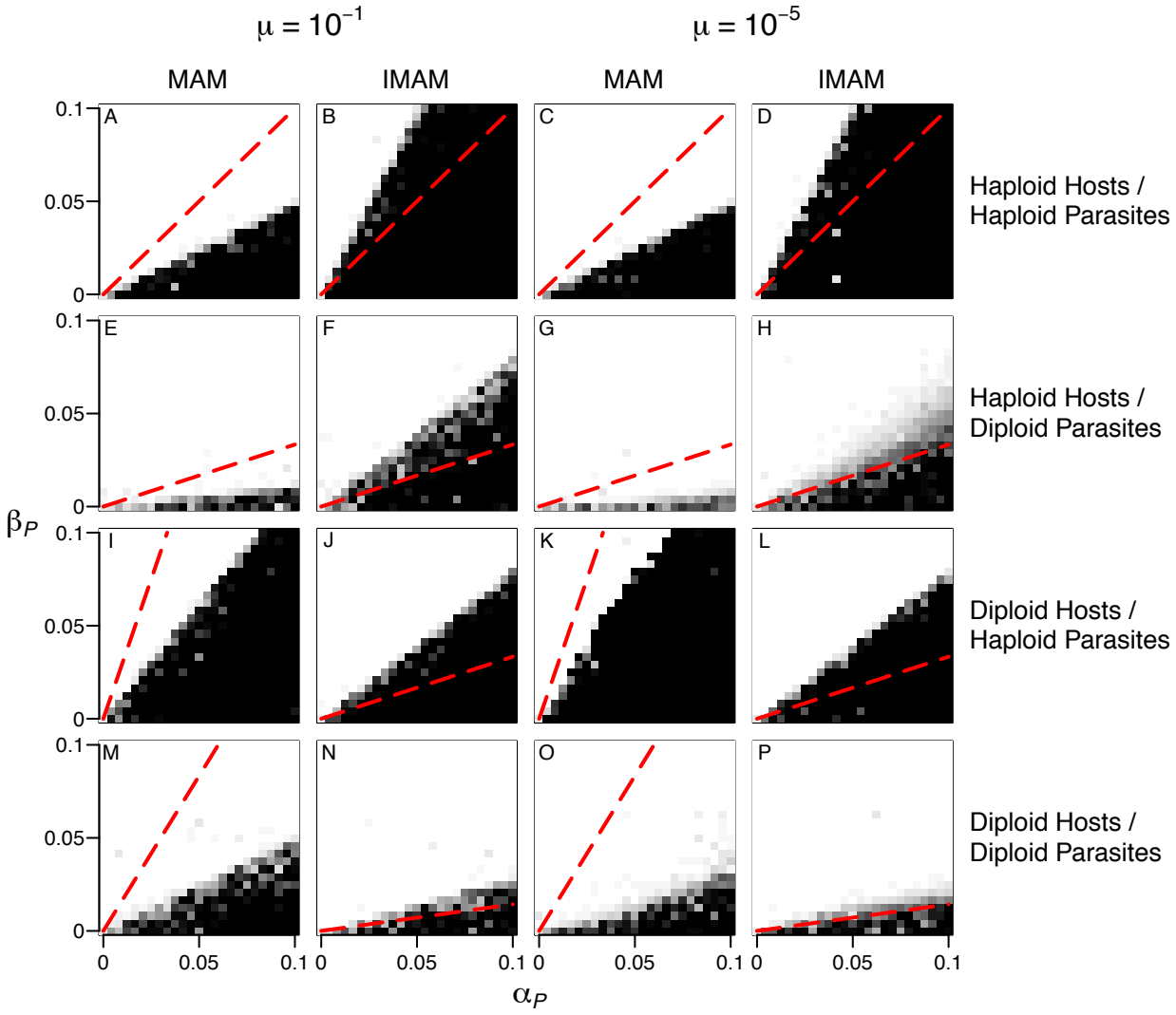

Figure S7: Same as figure S1, except with three alleles at the A-locus in each species. Dashed red lines denote the analytical invasion condition for the two-allele case, as given in table 4, and are included for comparison.

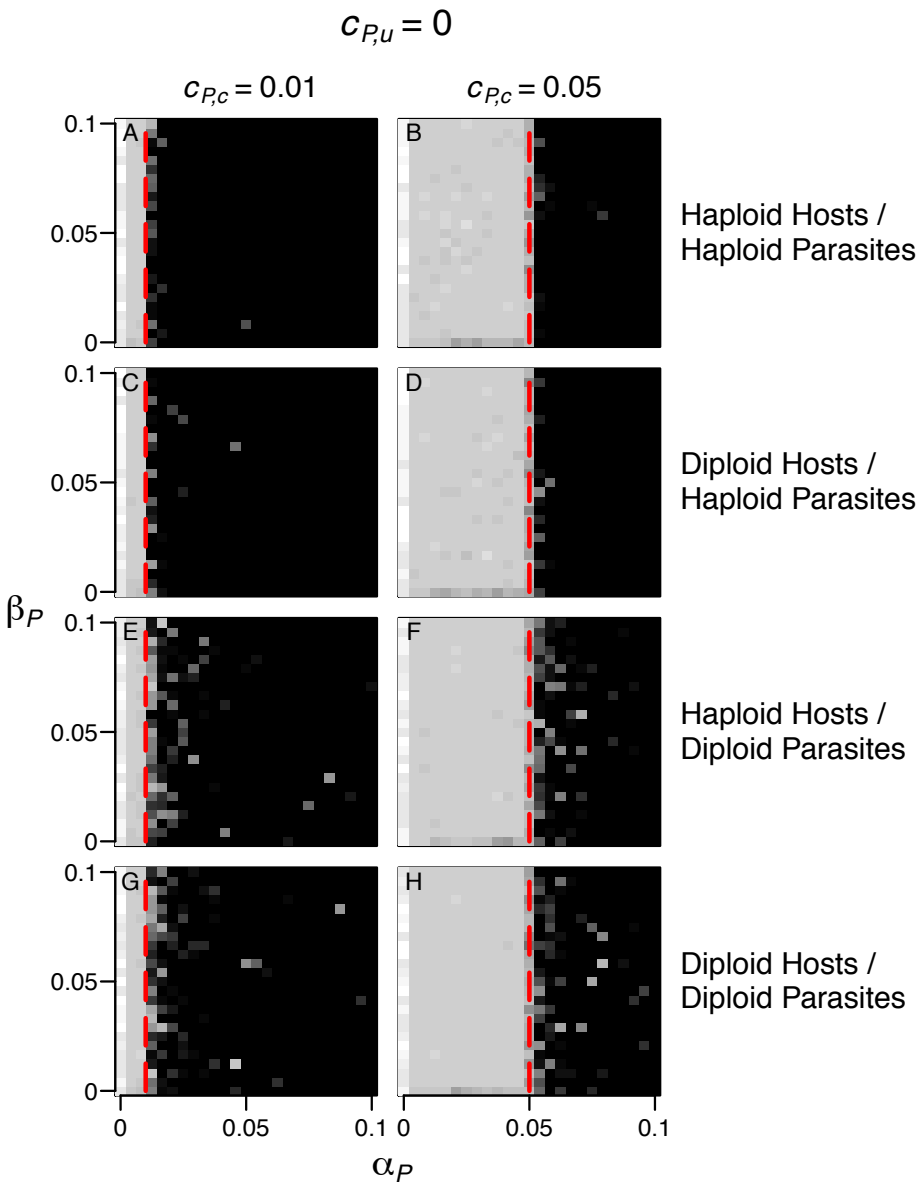

Figure S8: Evolutionary convergent level of parasitism (f) in the GFG with conditional costs to virulence, as indicated by column headings. Dashed red lines denote the value of α_P for which $\bar{w}_{\text{diff}}$ in eq. (6) is zero. Other parameters were as in figure S1, along with $\mu = 10^{-5}$ and $c_H = 0.01$.

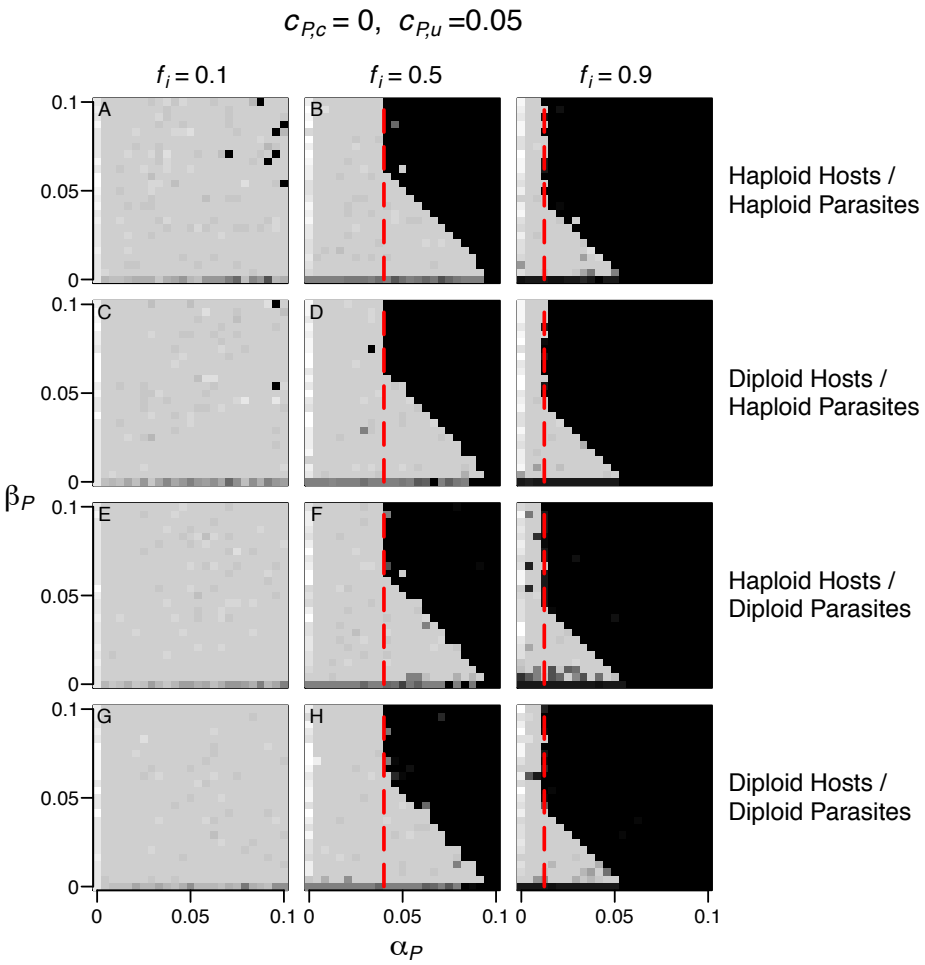

Figure S9: Evolutionary convergent level of parasitism (f) in the GFG with unconditional costs to virulence, and differing initial levels of parasitism, as indicated by column headings. Dashed red lines denote the value of α_P for which $\bar{w}_{\text{diff}}$ in eq. (7) is zero. The poor fit for small β_P (grey triangular regions to the right of the dashed red lines) is a consequence of selection being insufficiently strong to maintain the costly virulent allele, thereby reducing the advantage of being parasitic. Thus cycles do not occur and parasitism does not evolve. Other parameters were as in figure S1, along with $\mu = 10^{-5}$ and $c_H = 0.01$.

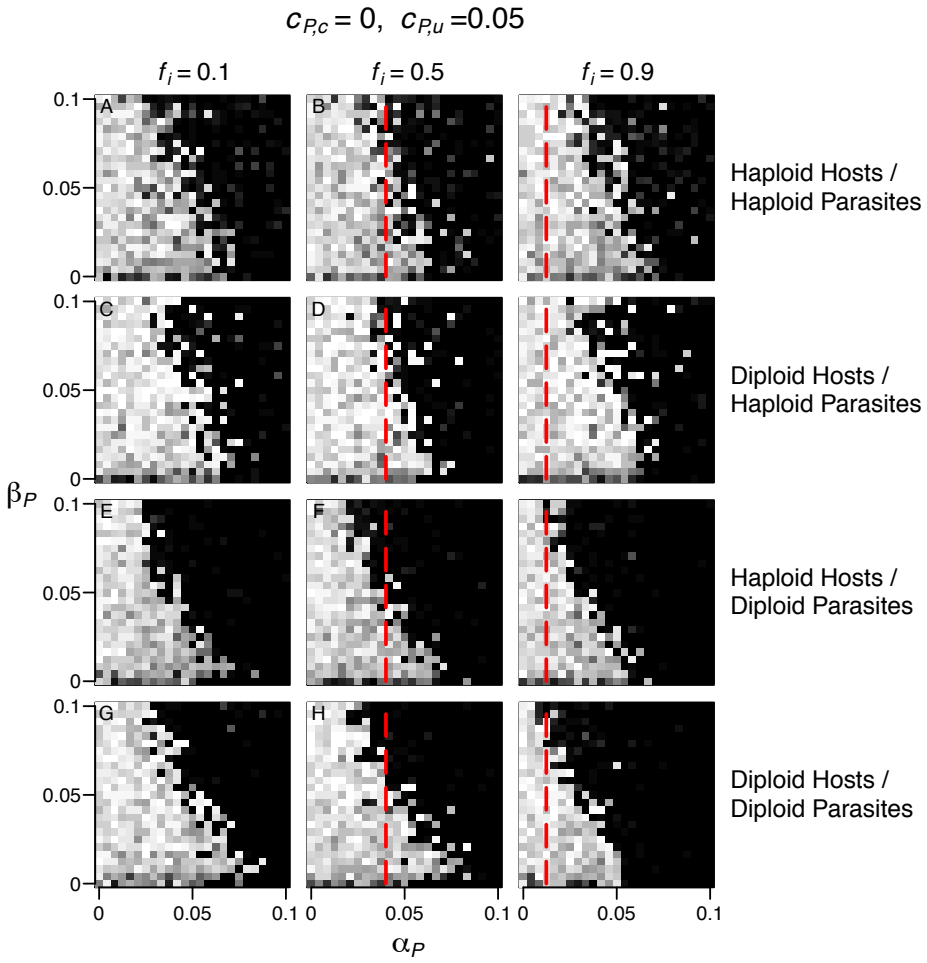

Figure S10: Evolutionary convergent level of parasitism (f) in the GFG with unconditional costs to virulence, differing initial levels of parasitism, and small populations. All parameters are as in figure S9, except population sizes were 10^3.